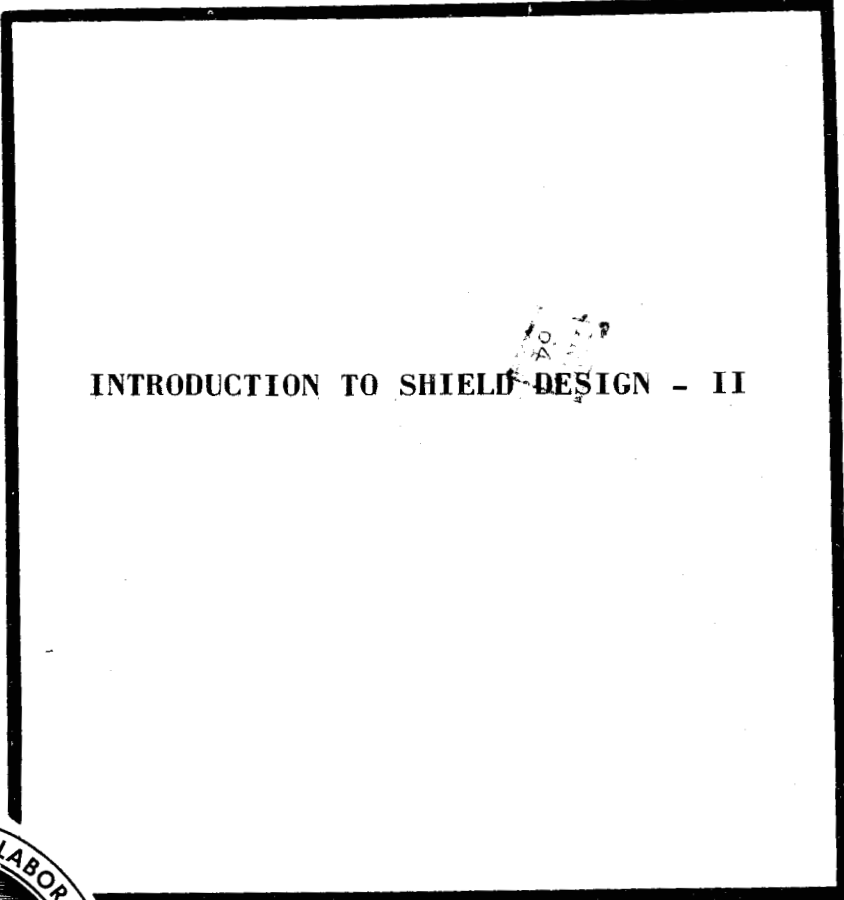
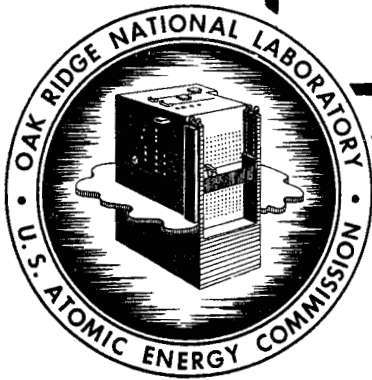


~~CONFIDENTIAL~~

ORNL
Central Files Number
51-10-70 - Part II
Revised



INTRODUCTION TO SHIELD DESIGN - II



OAK RIDGE NATIONAL LABORATORY
OPERATED BY
CARBIDE AND CARBON CHEMICALS COMPANY
A DIVISION OF UNION CARBIDE AND CARBON CORPORATION



POST OFFICE BOX P
OAK RIDGE, TENNESSEE

~~CONFIDENTIAL~~

~~CONFIDENTIAL~~

[REDACTED]

ORNL
Central Files Number
51-10-70
Part II
Revised

This document consists of 44 pages.
Copy 162 of 216. Series A.

OAK RIDGE NATIONAL LABORATORY

69
APR 7

INTRODUCTION TO SHIELD DESIGN - II

E. P. Blizard

Part II:

Comparison Method of Shield Design

CLASSIFICATION CANCELLED
DATE 10/7/65
For The Atomic Energy Commission
H. F. Canale
Chief, Declassification Branch TC

March 7, 1952

This article is to be the basis for a chapter in a Reactor Technology
textbook being edited by Samuel Glasstone and Neal F. Lansing.

[REDACTED]

[REDACTED]



Distribution - Internal

1. E. P. Blizard
2. R. C. Briant
3. C. E. Clifford
4. H. L. F. Enlund
5. A. P. Fraas
- 6-15. N. F. Lansing
16. F. K. McGowan
17. J. L. Meem
18. F. J. Muckenthaler
19. F. H. Murray
20. J. D. Flynn
21. T. V. Blosser
22. H. E. Hungerford
23. J. M. Miller
24. G. T. Chapman
25. F. N. Watson
26. R. G. Cochran
27. F. C. Maienschein
28. J. K. Leslie
29. G. M. McCammon
30. M. P. Haydon
31. M. K. Hullings
32. E. B. Johnson
33. K. M. Henry
34. R. H. Ritchie
35. A. Simon
36. A. H. Snell
37. A. M. Weinberg
38. E. O. Wollan
39. C. L. Storrs
- 40-89. Central Files
- 90-189. ORSORT Files
190. Physics Library





Distribution - External

- 191. H. A. Bethe - Cornell University
- 192. W. L. Carss - U.S.A.F. Oak Ridge
- 193. C. F. deGanahl - Pratt and Whitney Aircraft Corporation
- 194. J. R. Dietrich - Argonne National Laboratory
- 195. M. Fox - Brookhaven National Laboratory
- 196. K. Kasschau - AEC,
- 197. C. R. Horner - AEC, Washington, D. C.
- 198. E. O. Meals - AEC, Washington, D. C.
- 199. T. Rockwell - Bureau of Ships
- 200-202. J. R. Hood - Wright Patterson Air Force Base
- 203. B. F. Ruffner - Boeing Airplane Company
- 204. J. H. Smith - Knolls Atomic Power Laboratory
- 205. H. E. Stone - Knolls Atomic Power Laboratory
- 206. H. E. Stern - Consolidated Vultee Aircraft
- 207. F. A. Cleveland - Lockheed Aircraft Corporation
- 208. J. J. Taylor - Westinghouse Electric Corporation
- 209. A. F. Thompson - AEC, Washington, D. C.
- 210-211. G. Thornton - GE-ANP
- 212. L. Tonks - Knolls Atomic Power Laboratory
- 213. G. Young - NDA
- 214. R. Zirkind
- 215-216. Technical Information Service - AEC, Oak Ridge

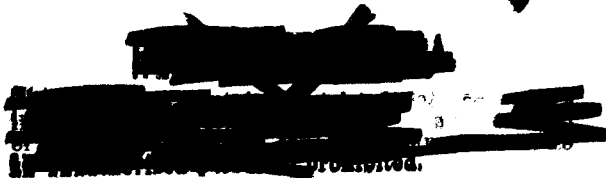


TABLE OF CONTENTS

INTRODUCTION TO SHIELD DESIGN - II

Part II	Page No.
A. COMPARISON METHOD OF SHIELD DESIGN	74
1. Introduction	74
2. Description of Experimental Facilities	74
a. ORNL Core Hole	75
b. ORNL Lid Tank	75
c. ORNL Bulk Shielding Facility	76
d. BNL Shielding Facility	79
3. Comparison of Source Strengths	82
a. Gamma Shielding by Comparison Method	94
4. Comparison of Different Materials	95
a. The Effective Neutron Removal Cross Section	95
b. Gamma-ray Shielding with No Secondary Production	97
c. Gamma-ray Shielding with Secondary Production	98
5. Estimation of Fast-Neutron Current from Thermal Flux in Water	100
6. The Biological Dose	107
7. Relative Biological Effectiveness	107
B. REFERENCES	111

List of Tables

Table No.	Title	
8	Gamma-ray Shields	98
9	Relative Biological Effectiveness	108
10	Neutron Fluxes Equivalent to 0.3 rep of Gamma Rays per 40-hr Week	110

ABSTRACT

The several shielding research facilities are described and the use of their data by comparison between experimental geometry, power, etc., with the design situation is explained. Relative effective source strengths are calculated. A simple method is shown for allowing for small amounts of different shield materials.

A simple method for estimating fast neutron dose from thermal flux in water is derived.

The biological effectiveness of the several radiations encountered in reactor shielding is listed.

- - - - -



COMPARISON METHOD OF SHIELD DESIGN (25-26)

Introduction

There are two commonly used methods of designing reactor shields. The present section is devoted to the so-called "comparison method," in which the data of a full-scale experiment are transformed by the methods in the previous section to the geometry of the reactor to be shielded so that a direct comparison in dose for a given power level is available. This is generally considered the most reliable method of design, but of course it has the drawback that in many cases there are no experiments which can be transformed to the desired situation, so that a new experiment is required. This eventually should become less and less common, however, as more shields are measured.

The second method of shield design, which will be the subject of a subsequent section, is based on calculations of a water shield, in which neutron collisions are treated as absorptions, with the exception that a buildup factor is later applied to account for the scattered component. Gamma-ray attenuation is calculated on the basis of a simplified picture which leads to a linear buildup factor. The secondary gamma rays are necessarily treated by a more laborious method.

The neutron cross sections to be used are obtained from the shielding experiments themselves, often the same experiments that are used for the comparison method. The direct calculation method is somewhat more flexible, but also probably less reliable. The uncertainties in buildup factor and secondary gamma production are fortunately not always small.

Description of Experimental Facilities

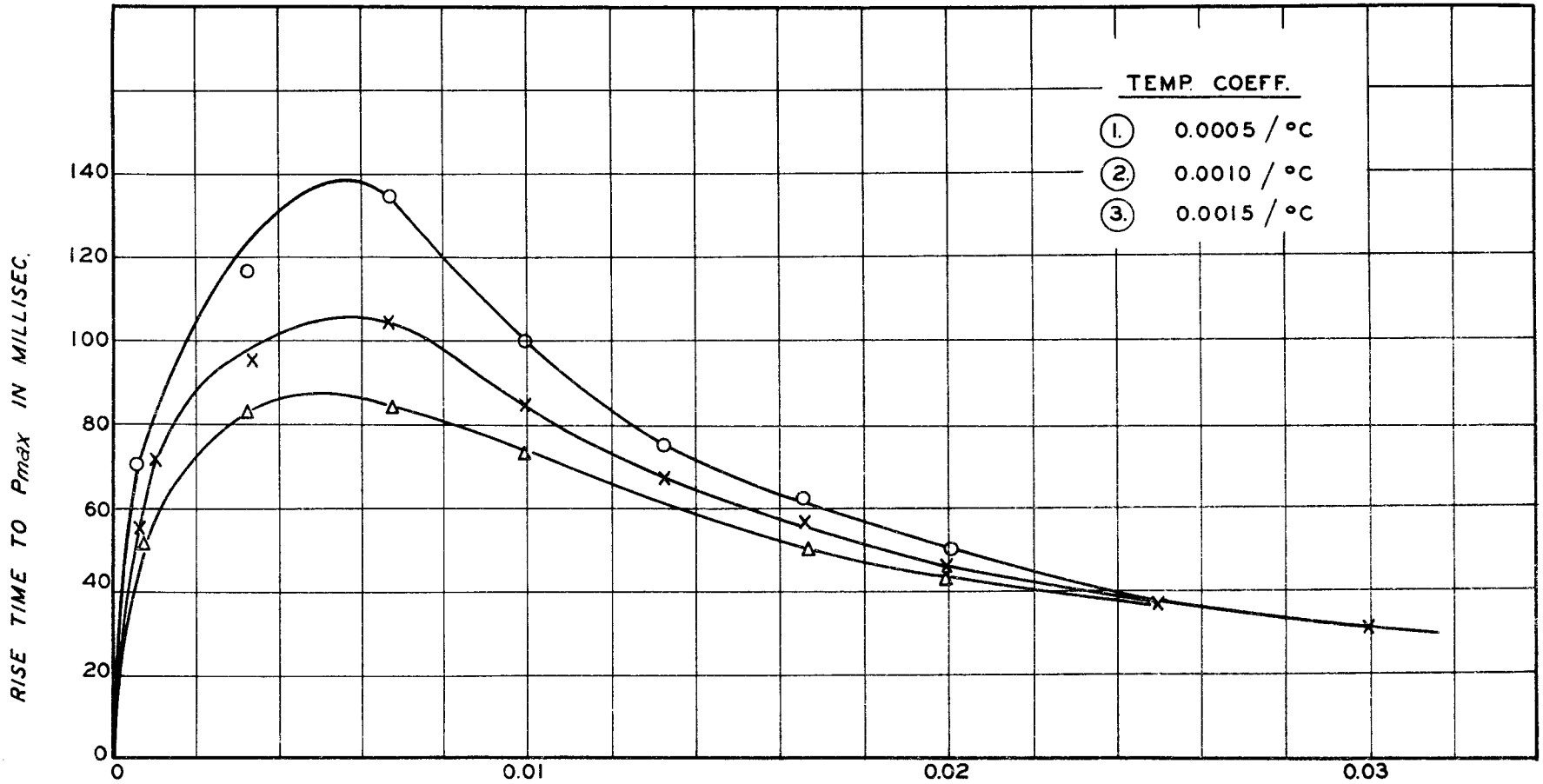
Since the "comparison method" requires a fairly complete knowledge of the experiments which are used, it is appropriate that the several facilities be described here.

ORNL Core Hole. (27-29) This is the oldest facility on which a shielding program has been based. It consists of a 2-ft. square hole through the 7-ft concrete shield of the Oak Ridge graphite reactor. Materials to be tested were inserted in this hole, considerable care being taken to insure a close fit. The source was the reactor itself, except that in one experiment (30) an array of uranium slugs was fastened to the inner sample face to insure a known source spectrum. Experiments were confined to concretes WC, B₄C, Fe, Pb, (31) and the Hanford iron-masonite shield.

In general the samples were too narrow, owing to the small size of the hole, so that radiation mixed considerably between the sample and the surrounding concrete. As a result there was considerable uncertainty in the interpretation of much of the data. There was a notable exception in the case of ordinary concrete, which matched the surrounding shield so well that the mixing had little effect. The data for this test (32) is still useful, even through no adequate theory has been devised for understanding it.

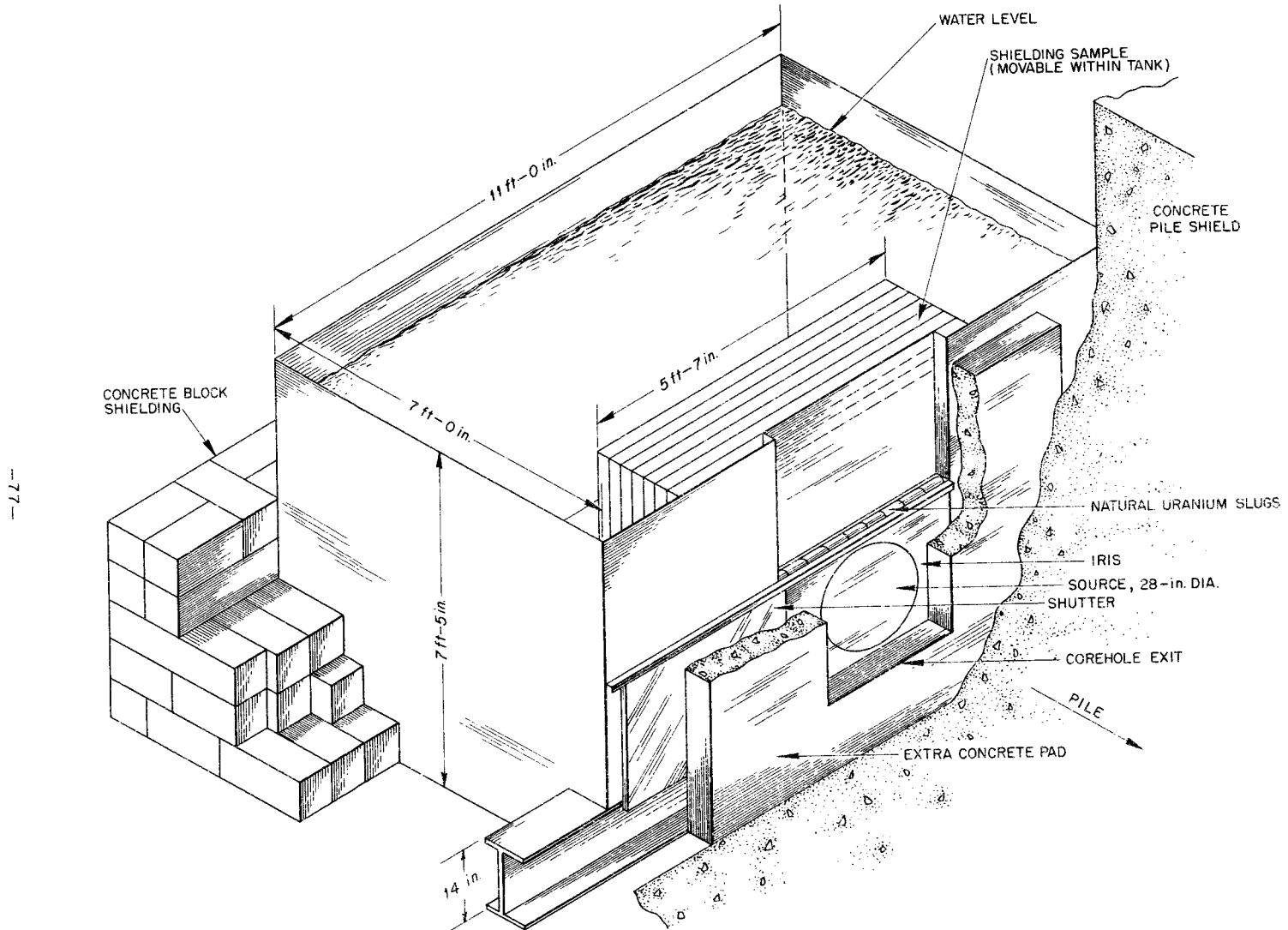
ORNL Lid Tank. (33) This facility, which makes use of and supersedes the core hole, has served as the work-horse of the AEC shielding program since its completion near the end of 1949. Its source is a circular plate of natural uranium (made up of X-10 slugs) placed over the outer end of the core hole. Thermal neutrons from the graphite reactor impinge on this uranium, causing fissions to take place. The fast neutrons and gammas so produced then enter a large tank of water, in which the shield to be tested is inserted. The facility receives its name from the fact that the tanks fits as a lid over the core hole. Figures 15 and 16 show the layout.

Measurements are made in the Lid Tank with a variety of instruments in the water behind the various shields. Although this is somewhat inconvenient in that the instruments must be made waterproof, this disadvantage is easily



$\frac{\delta K_e}{K}$ STEP FUNCTION

FIG. 15
RISE TIME VS. δK



77-

Fig.16 Isometric View of Lid Tank.

overcome and is far outweighed by the advantages, among which are the following:

1) The background counts, due to pile leakage, etc. are considerably reduced by the water, so that very low intensities can be measured at the outside of the shield samples.

2) The attenuation in water gives some indication of the spectrum of radiation penetrating the shield sample.

3) Water is a very convenient integrator of fast-neutron flux, since it moderates quickly to the thermal energy region where measurements are much more easily taken.

4) Many shields incorporate water as a dominant component, especially in the outer regions. These are very easily mocked-up in the Lid Tank.

The source power has been measured by observing the temperature as a function of time on opening and closing a boron shutter. The value so obtained was 6 watts. The effective area is 3970 cm². It is covered by several items such as source box walls, water tank wall (a lead sheet is used where the radiation enters), the shutter assembly, etc. These items introduce a total attenuation of fast neutrons of about 5/3, so that the measured source strength must be reduced by a factor of 0.6. One advantage of the Lid Tank is this large neutron leakage factor, which not only means good intensity for measurements, but also implies relatively little uncertainty in source strength (the factor cannot exceed 1, and cannot be much less than the measured 0.6).

ORNL Bulk Shielding Facility. (34-35) This is the first facility in which a reactor has been used primarily for shielding research. The need for such a facility became evident when the intensity in the Lid Tank proved too low for fast-neutron dose measurements at full shield thicknesses. (36-37)

Figure 17 shows the general layout of the facility, and in Figure 18 its use in the measurement of a shield is illustrated. The equipment comprises primarily a small low-power MTR-type reactor suspended in a large pool of water. The water acts as coolant, moderator, reflector, and shield. The shields are inserted next to, underneath, or around the reactor. Where possible the water of the pool serves as part of the mockup. Thus measurements in the water of the pool give data on all-water reactor shield.

Although the Bulk Shielding Facility lacks the simplicity of the Lid Tank, it nevertheless offers many advantages, to wit:

1) At 10-kw power it just provides sufficient intensity for spectroscopic studies behind full thickness aircraft reactor shields. At 100 kw, which could be achieved with minor modifications, the situation would be even better*.

2) It makes possible the measuring of shields with curvature in the layers, obviating the geometry transformations that are used in applying Lid Tank slab-shield measurements to small reactors.

3) It is operable over a wide range of powers, so that the same detector can be used throughout large attenuations.

4) The advantage of low background, due to the fact that the measurements are taken within the water, is even more pronounced in this case, since there is so much more water -- 17 ft from reactor top to pool surface.

BNL Shielding Facility.⁽³⁸⁾ This facility consists of a uranium source plate, irradiated by slow neutrons from the Brookhaven reactor and mounted just below a large tank of water which extends not only through the entire 5-ft shield thickness, but 7-ft above as well. Although this facility has not been put to much use at the time of this writing, it nevertheless offers some unique advantages over the ORNL facilities:

* Operation at 100 kw. was approved July, 1952 and operation at that power level has proved satisfactory.

DWG #8332

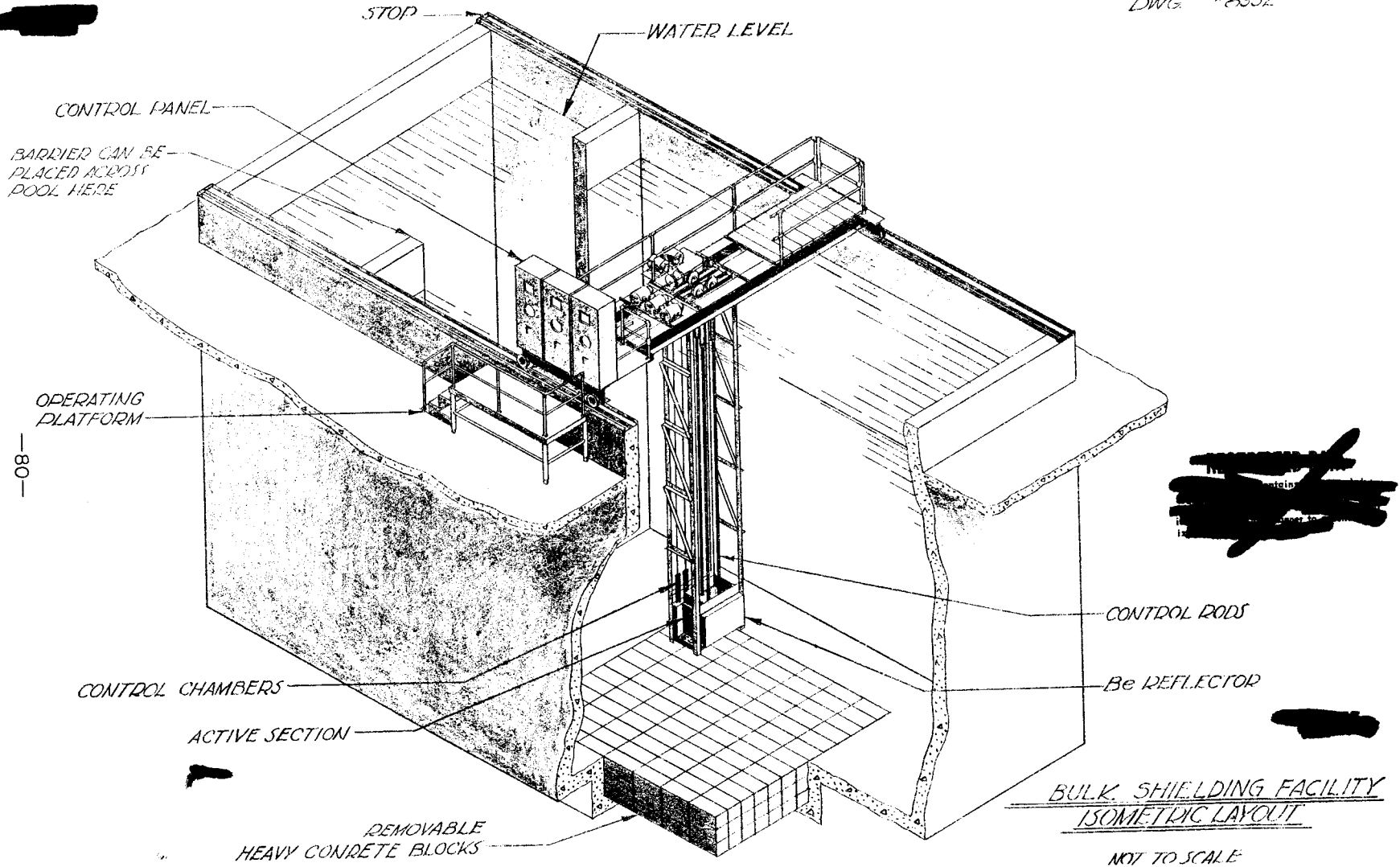


Fig. 17

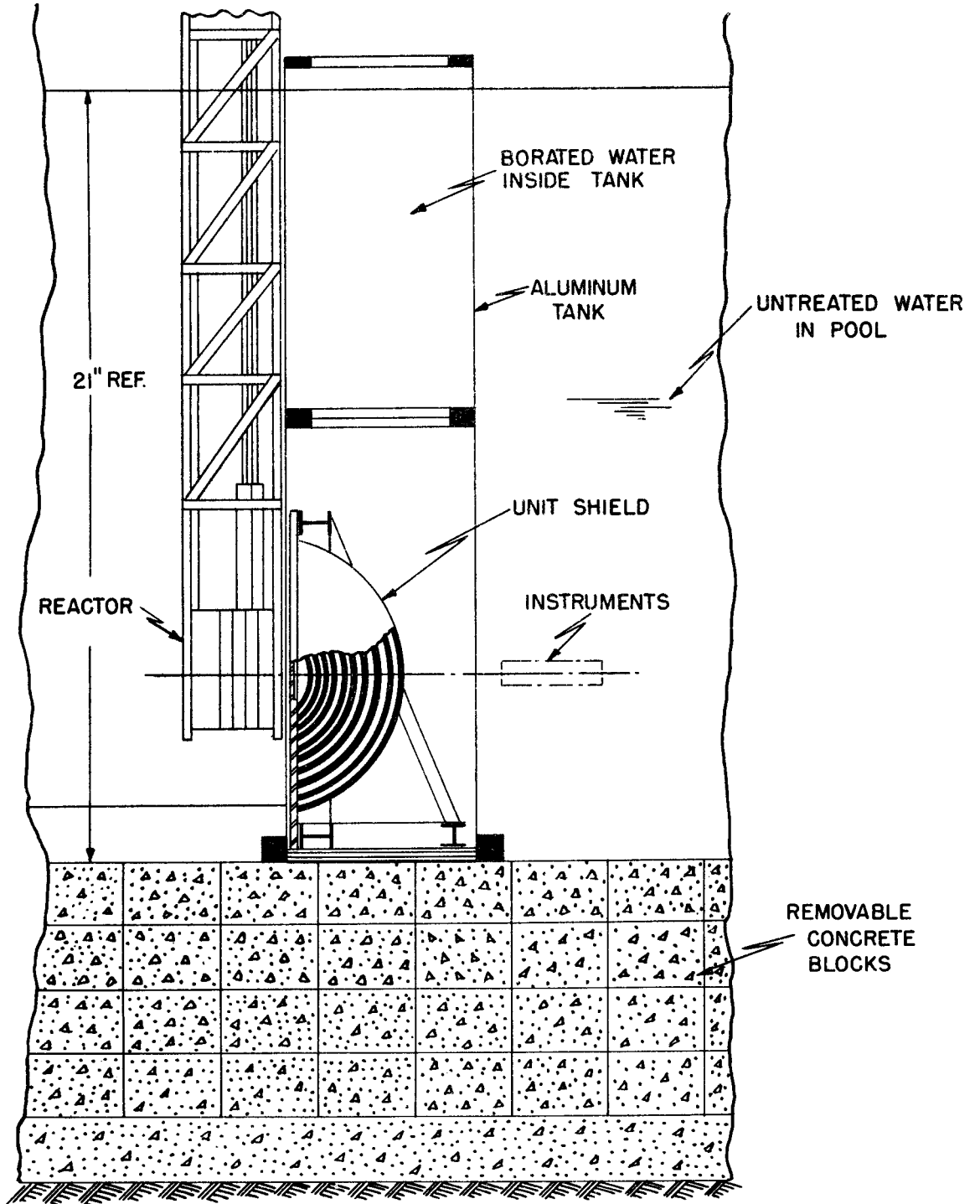


Fig. 18
UNIT SHIELD MOCK-UP
BULK SHIELDING FACILITY

- 1) The power level of the largest source plate (there are three) is about 750 watts, a factor of about 10^2 over the Lid Tank.
- 2) It offers a unique variability in that three sizes of source plate are available. This should be very useful in checking geometric effects, as well as affording different effective source strengths.

In addition, of course, it matches many of the advantages of the ORNL facilities, which have been mentioned already.

Comparison of Source Strengths

In order to compare the source which is used in a shielding experiment with that of an actual reactor, it is necessary to make some sort of estimate of the self-absorption in the two cases. Fortunately most of the radiation which leaks does so from the region near its periphery, so that it is quite adequate to calculate leakages using simple exponential attenuation. The core relaxation length can be either the mean free path or some better estimate based on comparison of cross sections and measured relaxation lengths. The section on effective removal cross sections, vide infra, described the latter. For the present a core relaxation length, λ_c , will be used for the attenuation in the reactive volume without specifying its origin.

It will be shown that to adequate accuracy the volume-distributed source can be replaced by a surface-distributed source which will give the same attenuated dose at the shield exterior. The relationship between the volume and surface source strengths will also be derived for two common power distributions.

Consider a small volume, dv , of the reactor, the rate of power dissipation therein being $p(x,y,z)dv$. The total of contributions of elements such as this to the dose at some observation point outside the shield is required.

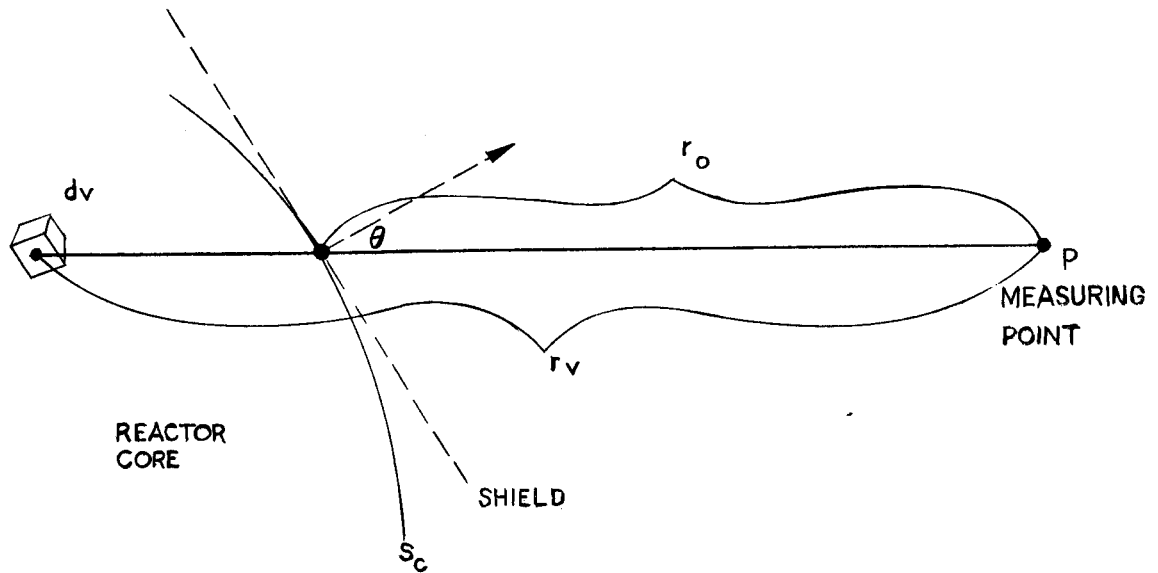


Figure 19

According to the assumption of simple exponential attenuation in the core, the dose read at P will be

$$D_p = A \int_{\text{core}} e^{-(r_v - r_0)/\lambda_c} \frac{g(r_0)}{4\pi r_v^2} p(r_v) dv, \quad (75)$$

where A is a constant conversion factor from power release to dose rate at unit distance shield and the function $g(R)$ is defined in terms of the point-to-point kernel $G(R)$ as follows:

$$G(R) = \frac{g(R)}{4\pi R^2}, \quad (76)$$

It is also seen from the figure that

$$dv = ds_c \cos\theta dr_v \left(\frac{r_v}{r_0}\right)^2 \quad (77)$$

where θ is the angle of r_0 with the normal to the surface and ds_c is the element of core surface. A simplification, that of replacing $\cos\theta$ by unity, is justified on the basis that for regions of large θ the distance r_0 is so increased that the contribution to the dose will be small.

The foregoing simplifications result in the following:

$$D \cong A \int_{s_c} \frac{g(r_o) ds_c}{4\pi r_o^2} \int_{r_v = r_o}^{r_v \cong \infty} e^{-(r_v - r_o)/\lambda} p(r_v) dr_v. \quad (78)$$

The upper limit for r_v is taken as infinity for simplicity. If the core diameter is larger than $2\lambda_c$, then this will introduce an error no greater than about 10%. This condition is usually well fulfilled. If it is not, then a method derived in connection with the "fast effect" is applicable. (39-41)

In reactors which are used for power production it is usually desirable to keep the heat release density, p , constant over the volume. For this case the second integral is easily evaluated. For

$$p(r_v) = p_o = \text{constant},$$

$$D_p = \text{const.} \cong \lambda_c p_o A \int_{s_c} G(r_o) ds_c. \quad (79)$$

In other words, for constant power density in the core the equivalent surface source strength is simply $\lambda_c p_o$ watts/cm², and

$$\sigma_{\text{equiv.}} = A \lambda_c p_o. \quad (80)$$

It might be noted at this point that Eq. (80) is at variance with the familiar result for leakage from the surface of a radioactive self-absorbing semi-infinite volume source, to wit $N_o \lambda / 4$ particles per unit source area per unit time, where N_o is the activity per unit volume. The difference lies in two places. In the present discussion a milligoat detector is used, which would read $N_o \lambda / 2$, which is not the leakage at all. The second difference arose from the neglect of the cosine factor in Eq. (23). This means that Eq. (80) describes a source which is isotropic but matched to the actual

cosine source in the normal direction. This makes only negligible error for thick shields.

For the case in which the power can be represented as a constant plus a cosine function the equivalence is again easily derived if the core diameter is large compared to λ_c :

$$p(r_v) = p_0 + p_1 \cos \left[\frac{\pi}{2} \left(1 - \frac{r_v - r_0}{a} \right) \right] \quad (81)$$

$$= p_0 + p_1 \sin \left(\frac{\pi}{2} \frac{r_v - r_0}{a} \right), \quad (82)$$

where a is the core half-width.

Equation (81) can be approximated near the core surface, using the argument to replace the sine by the following expression:

$$p(r_v) \cong p_0 + p_1 \frac{\pi}{2a} (r_v - r_0). \quad (83)$$

For this case, Eq. (78) becomes

$$D p_0 + p_1 \cos () = A \left(\lambda_c p_0 + p_1 \frac{\pi \lambda_c^2}{2a} \right) \int_{s_c} G(r_0) ds_c, \quad (84)$$

$$\sigma_{\text{equiv.}} = A \left(\lambda_c p_0 + \lambda_c^2 \frac{\pi}{2a} p_1 \right) \quad (85)$$

The source strengths represented by Eqs. (80) and (85) are appropriate for use with the transformations in the previous section.

The evaluation of A is fortunately not necessary in the pure comparison method, for A is of course not a function of geometry and hence is the same for experiment as for the design reactor.

Example: 1) Neutron Shielding by Comparison with BSR

Leakage calculations are illustrated by the following example:

Reactor

Shape: Spherical, radius 60 cm.

Power:

$$p(r) = 100 + 127 \cos \frac{\pi r}{2a}, \text{ watts/cm}^3 .$$

(This corresponds to about 10^8 watts total and is adjusted so that peak power density is just twice the average.)

$$\lambda_c = 10 \text{ cm}$$

Shield

water

Experiment

Data: Bulk Shielding Facility data, Fig. 20.

Reactor for experiment:

Shape: rectangular parallelepiped, 24 x 15 x 15 in.

Power: Fig. 19 data is normalized to 1 watt.

Power density: to be assumed constant over volume
and equal to 1.13×10^{-5} watts/cm³
at one watt power level.

Relaxation length in BSR core = 9.7 cm.

It is required to find the thickness of water which will be necessary to reduce the fast-neutron dose at 50 ft from reactor center to 1/4 R/hr, which is equivalent to 1/40 rep/hr.

Treatment of the BSF reactor requires either considerable computation or, for reasonable accuracy, careful application of approximations. We shall indulge in the latter.

Let us choose as a hypothesis that we can neglect the lateral extent of the reactor, taking account only of self absorption due to its depth along the reactor-detector axis. At, say, 120 cm separation between detector and the nearest reactor face, what is the distance to the corner of the reactor, for which our approximation is worst? The distance is given by

$$L = \sqrt{120^2 + (7.5 \times 2.54)^2 + (12 \times 2.54)^2} = 125 \text{ cm.}$$

This means that the radiation from this corner must travel through an extra 5 cm of water and thereby will be reduced in intensity by a factor of about 1.7. This is too much, and we therefore look for the next approximation.

Suppose the contribution of each element of reactor face is reduced exponentially with the distance in excess of z , the basic distance (120 cm). (It is permissible to neglect the added geometric attenuation.) The intensity is then as follows (see Fig. 21):

$$D(z) = 4\sigma G(z) \int_{x=0}^a \int_{y=0}^b e^{-\frac{1}{\lambda} \left[\sqrt{z^2 + x^2 + y^2} - z \right]} dx dy .$$

Here λ can be taken from Fig. 20 in the region of 120 to 140 cm. Making use of the fact that $z \gg x, y$, it is easy to show that

$$\begin{aligned} D(z) &\approx 4\sigma G(z) \left[a - \frac{a^3}{6\lambda z} \right] \left[b - \frac{b^3}{6\lambda z} \right] \\ &\approx \sigma G(z) \left[4 ab \left(1 - \frac{a^2 + b^2}{6\lambda z} \right) \right], \end{aligned} \quad (86)$$

where $4 ab$ is the face area, σ is the surface strength, A is the usual constant to convert from power release to dose rate at unit distance, and $G(z)$ is the usual point-to-point kernel. The factor $\left(1 - \frac{a^2 + b^2}{6\lambda z} \right)$ indicated the

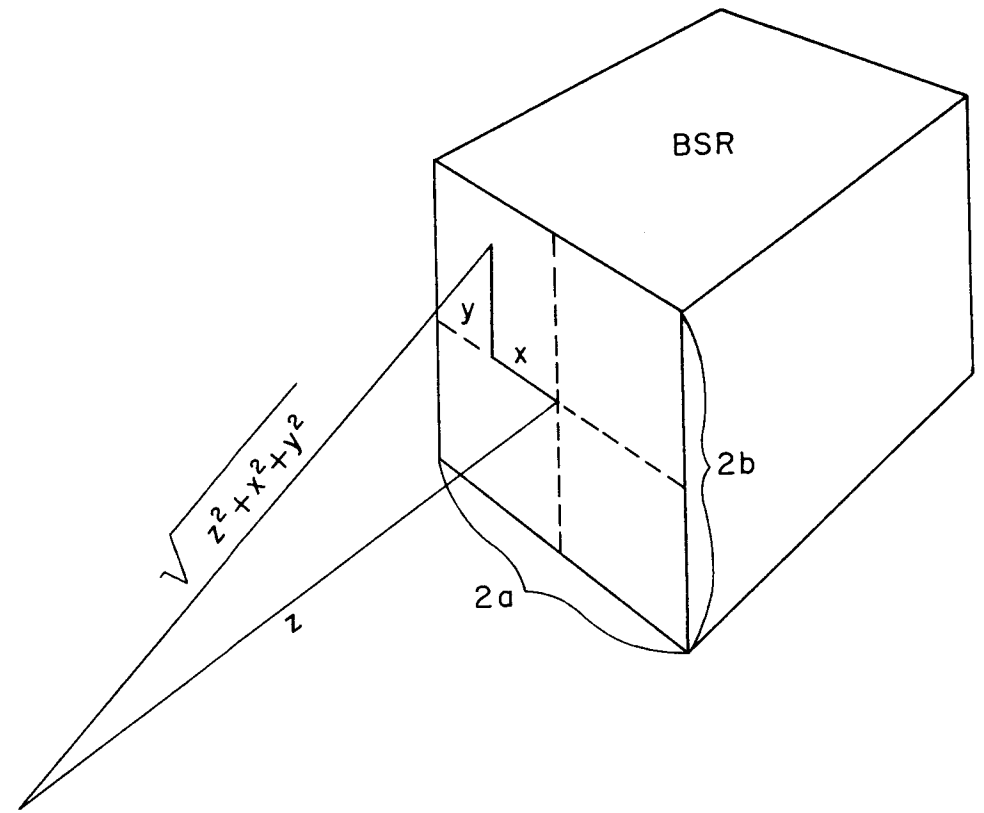


Fig. 21 Geometry For BSF Leakage Calculations

reduction in intensity at z due to the fact that parts of the reactor surface are farther than z from the detector. This factor becomes, for the case in point, about 0.80 and does not change appreciably in the range of interest.

If we now use Eq. (80) for the BSR, $\sigma = A\lambda_{BSR} P_{BSR}$, and Eq. (86) gives the following expression:

$$\begin{aligned} A G(z) &= \frac{D(z)}{9.7 \times 1.13 \times 10^{-5} \times 24 \times 15 (2.54)^2 \times 0.8} \\ &= 4.9 D(z), \text{ rep/hr/watt.} \end{aligned} \quad (87)$$

Since $D(z)$ is available from Fig. 20, we are now ready to make use of this data in designing the shield. As was mentioned before, A need not be evaluated, as it is the same for the BSR and the reactor for which we are designing a shield.

From Eq. (85) we find the equivalent surface strength of the reactor in question. From the specifications,

$$\begin{aligned} p(r) &= 100 + 127 \cos \frac{\pi r}{2a} \text{ watts/cm}^3 \\ \sigma_{\text{equiv.}} &= A \left(10 \cdot 100 + (10)^2 \cdot 127 \frac{\pi}{2 \cdot 60} \right) = 1332 A. \end{aligned}$$

From Eq. (33), (22), and the above,

$$\begin{aligned} D_s((60+z), 60) &\cong \frac{60}{60+z} \cdot 2\pi (1332A) \int_z^\infty G(R) R dR \\ &\cong \frac{60}{60+z} \cdot 2\pi (1332)(4.9) \int_z^\infty D(z) z dz. \end{aligned} \quad (88)$$

The integral is evaluated approximately by direct integration, after fitting $D(z)$ in the region of interest ($z \approx z_0$) by an exponential:

$$D(z) = D(z_0) e^{-(z - z_0)/\lambda} \quad (89)$$

For the required condition of $\frac{1}{40}$ rep/hr at 50 ft, we must have, by the inverse square law,

$$D_s(60 + z, 60) = \left(\frac{50 \times 30.5}{60 + z} \right)^2 \times \frac{1}{40} \text{ rep/hr} .$$

The required value of z , the shield thickness, is then determined by solution of the following equation:

$$.025 \left(\frac{50 \times 30.5}{60 + z} \right)^2 = \frac{60}{60 + z} \cdot 2\pi (1332)(4.9)(z\lambda + \lambda^2) D(z) \quad (90)$$

λ is of course specified by the requirement that Eq. (89) fit the data in Fig. 20. z is found, by trial and error, to be 144 cm.

It is often convenient to have a short-cut method, not necessarily very accurate, to check the results of the long calculation above. Such a method in this case would be to neglect the disparity in reactor shapes and relative core absorption, comparing directly on the basis of power density near the periphery. We illustrate this procedure by repeating the above problem:

$$D(z)_{\text{expt.}} = .025 \text{ rep/hr} \cdot \frac{1.13 \times 10^{-5} \text{ watts/cm}^3}{100 \text{ watts/cm}^3} \left(\frac{50 \times 30.5}{z + 60} \right)^2 \quad (91)$$

$$D(z)_{\text{expt.}} (z + 60)^2 = 6.59 \times 10^{-3} \quad (92)$$

Equation (91) says that the dose at the edge of the shield in the experiment should be equal to that allowed in the crew compartment (.025 rep/hr), corrected for the relative specific powers of the two reactors $\frac{1.13 \times 10^{-5} \text{ watts/cm}^3}{100 \text{ watts/cm}^3}$, and corrected for the fact that the crew

is 50 ft. away $\left(\frac{50 \times 30.5}{z + 60}\right)^2$. Eq. (91) is solved by $z = 142$ cm, not a bad estimate considering how easily it was obtained.

Example: 2) Neutron Shielding by Comparison with Lid Tank Data⁽²⁵⁾

Since a great deal of shielding information has originated in the ORNL Lid Tank, and since considerably more is expected both from this and the similar Brookhaven facility, it is profitable to study the conversion of this data to a pertinent design. The procedure is illustrated by the following example:

Reactor

Shape: cylindrical, height = 100 cm,

radius = 50 cm,

Power density: constant radially,

$$p(y) = 50 + 60 \cos(\pi y/2a) \text{ watts/cm}^3;$$

y is distance from median plane with core

ends at $y = \pm a$.

$$\lambda_c = 10 \text{ cm}$$

Allowed dose: .025 rep/hr at 1000 ft. from reactor.

Shield

Water with 1/2% B by wt.

Lid Tank

Data: see Fig. 22

Power: 6 watts total.

Self-shielding factor: 0.6.

Source shape: circular disc.

Size: radius = 14" = 35.6 cm,

area = 3970 cm².

It is required to specify how much shielding is required for the base of the reactor. By comparison, we can write down the following:

$$D_{L.T.}(z) = .025 \times \left(\frac{100 \times 30.5}{z + 50} \right)^2 \times \frac{6 \times 0.6 / 3970 \text{ watts/cm}^2}{50 \times 10 + (10)^2 \frac{\pi}{2 \times 50} \cdot 60} \times \frac{h(z, 35.6)}{h(z, 50)} \text{ rep/hr} \quad (93)$$

where the factors on the right are, in order:

- 1) The allowed dose in the design situation.
- 2) The correction for reactor-crew separation.

This is not exact since of course the reactor is not a sphere so the inverse square law is not directly applicable. The error involved is, however, not very much.

- 3) The ratio of surface source strengths, the numerator being that of the Lid Tank as shielded by its structure, the denominator being obtained directly from (85).
- 4) Hurwitz corrections for disc sources of the indicated radii. Each factor corrects to an infinitely large disc so that the two are then directly comparable.

Solution of Eq. (93) using Fig. 22 yields a shield thickness of about 88 cm.

Gamma Shielding by Comparison Method. The application of the comparison method to the design of shielding for gamma rays is somewhat more complicated because of the secondary production within the shield.

For the gammas which are produced within the reactor the methods of the preceding section apply, provided, of course that the relaxation lengths are not too long. This situation does not arise very often, so we will not treat it here. Suffice it to say that an upper limit to source strength can

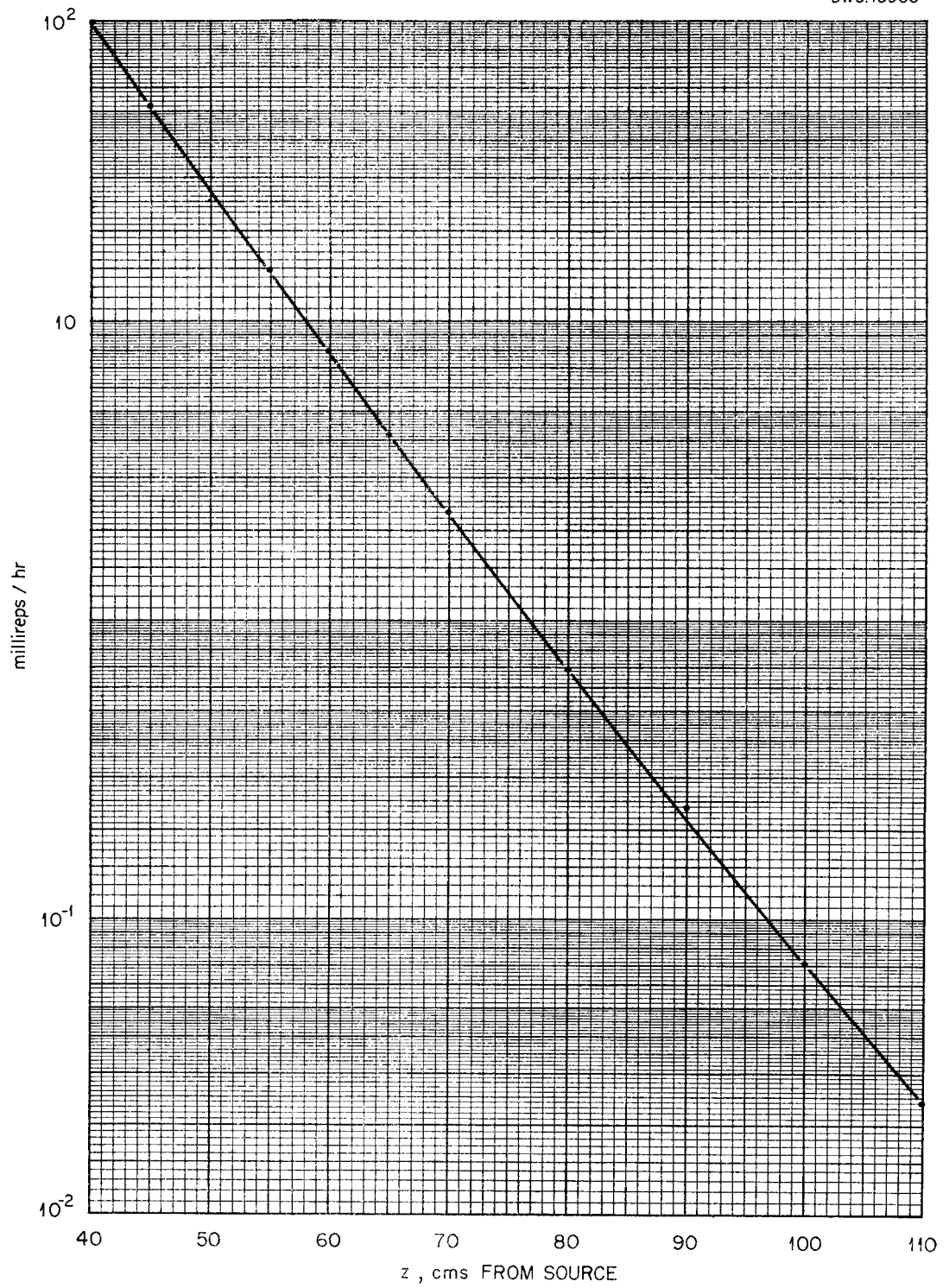


Fig.22 Fast Neutron Dose in Borated Water (½% B by wt.). ORNL Lid Tank data of Blizard, Clifford *et al.* from Physics Division quarterly report ORNL-919, p. 132. Data normalized to 6 watts power.

be had by ignoring the self absorption completely, and, if this is not adequate, then the methods of Murray⁽⁴⁰⁾ and others^{(39), (41)} can be resorted to.

In case the gammas are produced primarily in the shield, then the relative source strengths are just the same for neutrons and gammas, and the core relaxation lengths for neutrons are to be used for comparing gamma intensities.

For the Hurwitz transformation in the case of secondary gammas the gamma and not the neutron relaxation lengths are to be used since these determine the behavior at large distances.

Comparison of Different Materials

Although it is of course safest to perform an experiment on as exact a mockup as can be built, nevertheless this procedure is not often practicable, so that substitutions must be accepted. As a consequence it is important to know the effect of replacing one material with another in a shield. This cannot always be predicted with assurance, but there are certain situations in which we can do so with confidence. We shall now explore a few of these.

The Effective Neutron Removal Cross Section. Consider a water shield. Collisions of fast neutrons on hydrogen result in energy degradation with consequent increased probability per unit path length for the next collision. This is of course due to the increase in hydrogen cross section with decrease in neutron energy. As a consequence, as has been mentioned before, collision with hydrogen is tantamount to removal from the penetrating beam. This is not to say that there is not some biological effect due to the presence of these degraded neutrons, requiring the use of a buildup factor. This is indeed the case, but the factor is not large.

Collisions with oxygen are not, on the other hand, nearly so likely to result in removal of the neutron. There are two reasons for this. Firstly

the energy is not degraded very much unless the collision is inelastic, and secondly the elastic scattering, which might be expected to deflect the neutron into a direction in which its chances of penetration were small, is mostly in the forward direction, giving rise to a smaller removal effect. Nevertheless, it is possible to calculate with reasonable accuracy the penetration of a water shield on the basis of simple exponential attenuation using the total cross section of hydrogen and some effective removal cross section for oxygen⁽⁴²⁾. A small buildup factor must also be used, as indicated above.

Likewise other materials which are introduced into a water shield also exhibit effective removal cross sections. Some of these have already been tabulated on page 28. It is possible, by inference from nuclear radii to estimate the effective removal cross sections of many elements other than those which have been measured. This process has been discussed in some detail by Blizard and Welton,⁽¹⁶⁾ and the method has been applied in the preparation of the Report of the Shielding Board⁽⁴³⁾. The number of cases in which effective removal cross section and nuclear radii have both been measured is still, however, quite small. As a consequence no table such as that in the Shielding Board Report is prepared for the present text. Perhaps by the time a new edition is turned out this will be possible*.

The removal cross sections on page 28 are to be used for fast neutron removal in a shield which has adequate hydrogen to keep the dose from lower energy neutrons from being excessive. Just how much hydrogen this is, has never been properly determined, but concretes which are only 10% water by weight seem to be adequately so endowed. Of course oxygen, which makes up a large part of all ordinary concretes, is something of a moderator in its own right, so this 10% figure may not be too surprising. It has been demonstrated

* Aluminum has recently been measured to be 1.54 b.

that a pure iron shield will not work,⁽⁴⁴⁾ for the reason that intermediate energy neutrons, too low for inelastic scattering and too high for capture, are not appreciably attenuated and give large neutron currents. Even were these not themselves important biologically (they could, for example, be attenuated quickly by a little water), they would constitute a rather excessive source of secondary gammas at the outside of the iron. This last point is one of the most important points in all mobile shield design work, and it constitutes one of the commonest nemeses of the inexperienced.

Gamma-ray Shielding with No Secondary Production. Often a layer of gamma-ray shielding is introduced in a region of low neutron flux but high outward-bound gamma-ray flux. As a consequence the gamma rays produced by neutron capture or inelastic scattering within the layer are negligible, and the gamma-ray shielding materials considered for this layer can be compared on the basis of the total gamma ray cross sections which appear in Figs. 2 and 3. The photon energy at which the comparison is to be made depends on the source and the shield. If appreciable lead has been used, and if the source contains neutrons, then the appropriate energy is about 3 Mev, the minimum in the lead cross section curve, since the presence of neutrons usually assures a spread in energy of gammas up to about 7 or 8 Mev.

For convenience we include here the list of gamma ray absorption coefficients, or macroscopic cross sections which was used by the ANP Shielding Board and recorded in their report.

Table 8 Gamma-ray Shields

Element or Material	Density, gm/cm ³	Gamma Absorption Coefficient, μ , cm ⁻¹
Uranium	18.7	0.80
Lead	11.3	0.45
Gold	19.3	0.75
Tungsten	19.3	0.75
Iron	7.8	0.25
Aluminum	2.4	0.085
Sodium	0.93	0.033
B ₄ C	2.5	0.070
Lithium	0.53	0.014
Water	1.00	0.050
BeO	2.8	0.85

Gamma-ray Shielding with Secondary Production. Most high performance shields will incorporate gamma shielding at a location where the secondary gamma production in it is certainly not negligible. Since this involves introduction of an additional source to be shielded, this would seem at first glance to be poor practice. But for a given thickness of a layer of lead within a water shield, the weight is less the closer it is crowded in toward the core. The weight-saving incentive is balanced by the decrease in effectiveness due to secondary gamma production within the layer. As a consequence the optimum location is in a region where secondary production is important but not overwhelming. We shall discuss this process in more detail in connection with shield optimization.

In some shields, usually in connection with the optimization procedure, the effect of introducing lead into a water shield has been measured. This

effect can be expressed in terms of a "replacement length," " l ," which is measured as follows: A gamma ray detector is located at the shield exterior and a reading, Γ_1 , is taken. Then at a given location within the shield a layer of t cms of gamma material, say lead, is introduced, replacing water. A second gamma reading, Γ_2 , is taken. Then " l " is defined, analogously with the relaxation length, as follows:

$$l = \frac{t}{\ln \frac{\Gamma_1}{\Gamma_2}} \quad (94)$$

The relaxation length is perhaps easier to see from the following transformation of (94):

$$\Gamma_2 = \Gamma_1 e^{-t/l} \quad (95)$$

The l 's are functions of many variables, such as position within the shield, the total shield thickness, the source, and the composition of the shield throughout. Nevertheless they are often of considerable use in estimating the effect of small lead additions or removals on attenuation. The method is described in more detail in the Report of the Shielding Board. ⁽²²⁾

Problems 6.

It is desired to enhance the gamma attenuation of a spherical shield by a factor of 2 by the addition of a layer of lead. At the two radii which are convenient the l 's are measured, with results as follows:

- 1) at $r_1 = 90$ cms, $l = 4$ cms
- 2) at $r_2 = 120$ cms, $l = 2.3$ cms

How much lead (how thick) should be added at r_1 ? How much at r_2 ?

Which is better from the weight standpoint?

Estimation of Fast-Neutron Current from Thermal Flux in Water

Since it is much more difficult to measure fast neutrons than thermal neutrons, it is often necessary to forego the direct measurement and to estimate the biological dose due to fast neutrons from the measured thermal-neutron flux in a good moderator such as water. With instruments presently available this procedure increases the sensitivity of measurement by about 10^4 , although the method is not as accurate as the direct measurement when intensity is adequate. In the submarine shield attenuation tests this process has been mandatory, since the attenuations are so great that fast-neutron detectors are incapable of measuring directly the transmission of the shield mockups.

There is another important reason for making use of the thermal-neutron measurements, even in case the fast detector can also be used. The electronics of the fast-neutron recoil-proton dosimeter⁽⁴⁵⁾ are such that a definite cutoff in sensitivity must be used in order to discriminate against gamma rays. As a consequence, the instrument is blind to neutrons below the cutoff energy, which may be as high as a few hundred kilovolts. On the other hand the thermal flux indicates total neutron current regardless of energy. Even though it is possible to argue that neutrons below this cutoff energy will not contribute appreciably to the dose in most cases, it is nevertheless comforting to have at hand a technique which, in spite of its other limitations, does not possess this blind spot. Furthermore it is possible to conceive situations in which this low-energy component could be important, e.g. behind coolant ducts or with a large delayed neutron (low-energy) source. For these reasons it is clear that the estimation of fast-neutron current from thermal flux in water (or other highly hydrogenous media) will be important for some time.

Suppose a current of fast neutrons, of strength $I(z)$ $\text{cm}^{-2} \text{sec}^{-1}$ is traveling through water in the direction of increasing z . The question at hand is: What thermal flux will be observed as a result of this fast current? The neutrons are removed from the fast beam by collisions with the water atoms, slowed down in the water by many elastic collisions, and are absorbed as thermal neutrons by the hydrogen. Diffusion at thermal energy before absorption is taken account of separately by a slight adjustment of the slowing down length.

The rate of removal from the fast beam is easily calculated, since this is just the negative derivative of $I(z)$ with respect to z . These "removed" neutrons are then assumed to form a source for the slowing down process, which will be taken to be Gaussian. These slowed-down neutrons constitute the source for the thermal flux, which source must equal, under equilibrium conditions, the rate of thermal absorptions.

The foregoing process is represented by the following equation:

$$\Sigma_a \bar{\Phi}_{\text{th}}(z') = - \int_{z=0}^{\infty} \frac{dI(z)}{dz} q(z' - z) dz, \quad (96)$$

where $q(z' - z)$ is the probability that a fast neutron released at z with arbitrary initial direction will arrive at thermal energy at z' . q is of course a function of the initial energy as well as the properties of the moderator. If Gaussian slowing down is assumed, then

$$q(z' - z) = \frac{1}{\sqrt{4\pi\tau}} e^{-(z' - z)^2/4\tau} \quad (97)$$

where τ is the Fermi age for slowing down in water. This can be found for different energies in a report by N. Dismuke. ⁽⁴⁶⁾

In order to integrate the expression on the right of (96), it is necessary to make some assumption concerning the form of $I(z)$. This is done by assuming exponential behavior in the region of interest. Thus the true $I(z)$ is approximated in the region near z' as follows:

$$I(z) = I(z') e^{-(z - z')/\lambda}, \quad (98)$$

where λ , the relaxation length, is to be determined.

$$\frac{dI(z)}{dz} = -\frac{I(z')}{\lambda} e^{-(z - z')/\lambda}, \quad (99)$$

$$\Sigma_{a\downarrow th} \Phi(z') = \frac{I(z')}{\lambda \sqrt{4\pi\tau}} \int_{z=0}^{\infty} e^{-(z - z')/\lambda - (z' - z)^2/4\tau} dz \quad (100)$$

Let

$$\frac{z - z'}{\sqrt{4\tau}} = u, \quad dz = \sqrt{4\tau} du,$$

$$\frac{(z - z')^2}{4\tau} + \frac{z - z'}{\lambda} = (u + p)^2 - p^2,$$

where

$$2up = \frac{z - z'}{\lambda} \quad p = \frac{\sqrt{\tau}}{\lambda}$$

$$\Sigma_{a\downarrow th} \Phi(z') = \frac{I(z')}{\sqrt{\pi} \lambda} e^{\tau/\lambda^2} \int_{x = -\frac{z'}{\sqrt{4\tau}} + \frac{\sqrt{\tau}}{\lambda}}^{\infty} e^{-x^2} dx \quad (101)$$

The integral is just the error integral which is tabulated in many standard texts. ⁽⁴⁷⁻⁴⁸⁾ It is made up of two parts, as follows.

$$\int_0^{\infty} e^{-x^2} dx = \frac{\sqrt{\pi}}{2} \quad (102)$$

$$\int_{-m}^0 e^{-x^2} dx = \int_0^m e^{-x^2} dx = \frac{\sqrt{\pi}}{2} E(m) \quad (103)$$

where $E(m)$ is the tabulated function and m stands for the limit $\frac{\sqrt{\tau}}{\lambda} - \frac{z'}{\sqrt{4\tau}}$. Usually this limit is a large negative number; that is, the source is far from the point of measurement so that z' is large. As a consequence, the tabulated function is very nearly unity and the whole integral in (101) is just equal to $\sqrt{\pi}$. Thus

$$\Sigma_a \bar{\Phi}_{th}(z') = \frac{1}{\lambda} e^{\tau/\lambda^2} I(z') \quad (104)$$

or

$$I(z') = \lambda \Sigma_a \bar{\Phi}_{th}(z') e^{-\tau/\lambda^2} \quad (105)$$

The exponential term represents the attenuation to be expected in a distance τ/λ , so that (105) can be written as follows:

$$I(z') = \lambda \Sigma_a \bar{\Phi}_{th} \left(z' + \frac{\tau}{\lambda} \right). \quad (106)$$

The quantity τ/λ is referred to as the "displacement" between thermal and fast flux. It should be noted, however, that it is not the distance in water between places of equal thermal and fast fluxes, but rather it is the distance between places of equal removal rates for the fast and thermal neutrons.

Although (105) looks very pat, it is in effect not very accurate, nor is it immediately useful.

The choice of λ is not difficult, since it is clear that if λ and τ are not rapidly varying functions of z , then the relaxation length of the observed thermal flux will give a very good estimate of the corresponding quantity for the fast current.

Furthermore, the concept of a collimated fast-neutron current probably does not introduce serious errors since the most penetrating component is almost surely quite well collimated at large distances.

The source of "removed" neutrons, from which slowing down commences, however, was assumed by the form of (97) to be isotropic. This is definitely not the case. Collisions with hydrogen result in scattering through angles not over $\pi/2$. This means that the displacement is underestimated by this calculation.

Another difficulty arises in the choice of neutron energy for the purpose of determining \mathcal{T} . The energy before collision is certainly not appropriate, since the removal collision must introduce some moderation. The hydrogen collisions, which are usually the most frequent, result in energies which are uniformly distributed from zero to the initial energy. Choosing the initial energy for determination of \mathcal{T} overestimates the displacement, partially compensating for the error discussed in the preceding paragraph.

A third difficulty with the method compounds the two above. Although the penetration of fast neutrons is determined by the very high-energy beam, essentially uncollided, nevertheless there is carried along with this beam a much larger flux of intermediate energy neutrons, probably not more than two or three Mev, for which the displacement is small because of their lower energy and lack of collimation. These neutrons, representing the buildup in fast-neutron dose, account for nearly all of the measured dose but are not included in $I(z)$ as calculated, since no allowance is made for the dose due to partially slowed-down neutrons. It is the forte of the method that it is quantitatively accurate in counting neutrons, so that an adjustment of the displacement is adequate to make the method applicable.

To allow for these lower-energy less-collimated neutrons, an age corresponding to only about 3 Mev should be used. This choice makes equation (104) agree with the observed ratio of fast dose to thermal flux in those

regions in which intensity is sufficient so that both are measurable.* Note that while this adjustment must be made to λ , no such treatment is required for λ , which comes from the observed flux distribution in a straightforward manner.

The method just described can be considerably refined, making proper allowances for energy and direction in the collisions. One such attempt⁽⁴⁹⁾ gave a good estimate of the thermal flux in water from a fission-neutron source, but it has not yet been carried to the point of estimation of fast-neutron dose to be expected.

The thermal flux in the Lid Tank is shown in Fig. 23. It may be of interest to compare this with the data on Fig. 22.

Problem 7.

Choose one Lid Tank Curve and from this find the point-to-point kernel for that type of radiation. Plot this on the same graph.

Problem 8.

A cubic reactor, of sides 60 cms, is located in the middle of 12 ft. cube of water. It operates at 1000 watts total power, and the power distribution is given by the following expression:

$$p(x,y,z) = p_0 + p_1 \cos \frac{\pi x}{2a} \cos \frac{\pi y}{2d} \cos \frac{\pi z}{2a}$$

where $a = 30$ cms.

x, y, z are cartesian coordinates with origin at the center.

$$p_0 = p_1 .$$

* Incidentally this also accounts for the slightly greater displacement due to diffusion of neutrons after thermalization and before capture.

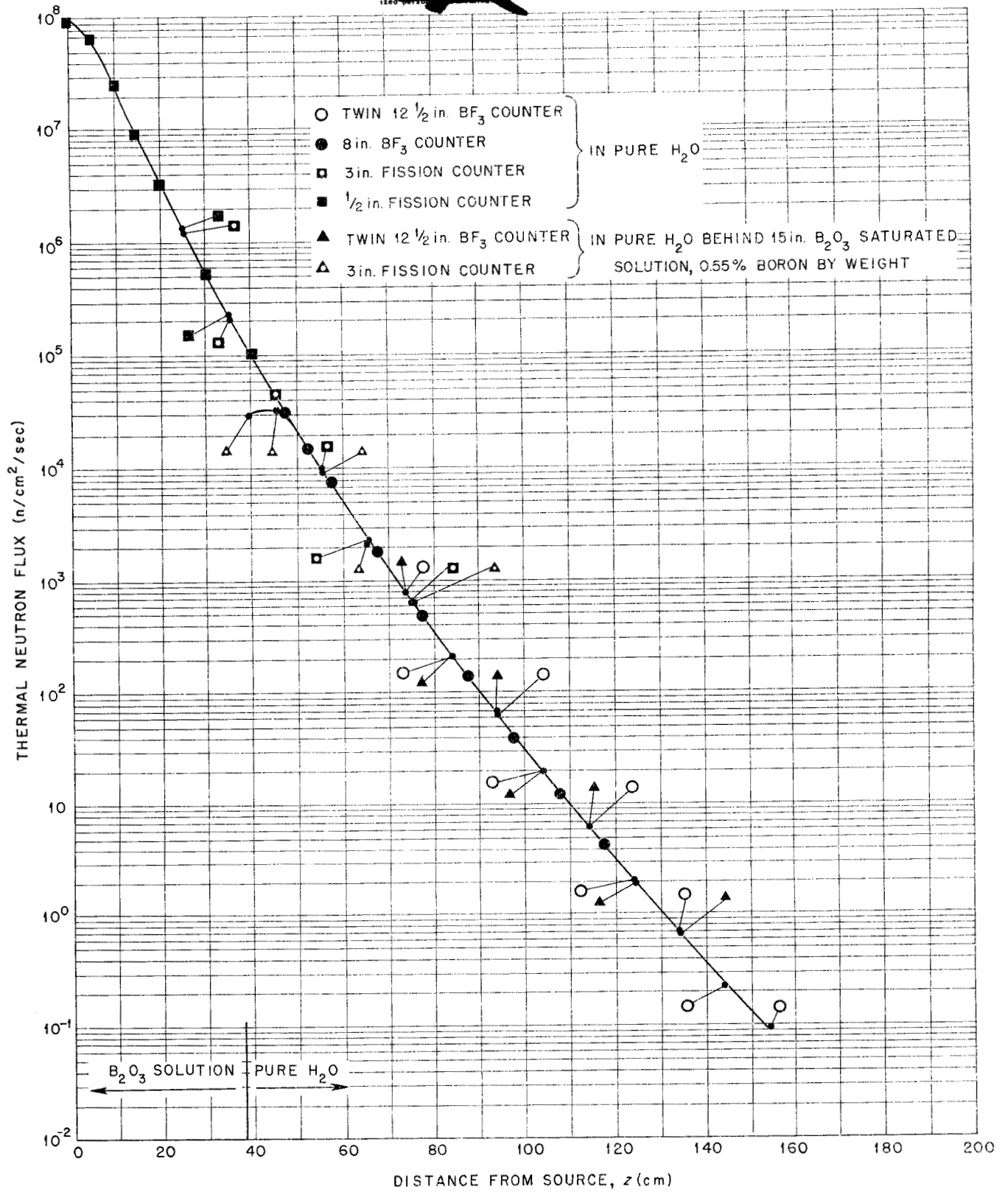


Fig. 23 - Thermal Neutron Flux in Water. ORNL Lid Tank Data.

What is the dose at the outside face center of the water shield for gammas and fast neutrons? Use the BSR data and assume uniform power distribution in the BSR.

The Biological Dose

The tolerable dose of radiation is still the subject of considerable research and not well-founded in fact. This is not surprising in view of the paucity of experience with radiation exposure of human beings. Nevertheless, in so far as the shield designer or the laboratory supervisor is concerned, the information is "legislated" where the research is yet undone. Consequently in the design of shields we accept certain tolerable doses which are specified or agreed upon. Much of this dogma comes from the "Permissible Doses Conference" of September 29-30, 1949, at Chalk River, Canada. This was attended by representatives of the United Kingdom, United States, and Canada. The minutes⁽⁵⁰⁾ are a valuable record of the decisions which were reached.

Relative Biological Effectiveness

The different types of radiation deposit their energy in the tissues in different ways, varying particularly in the energy density. As this affects the number of cells killed, for example, per erg deposited, it is necessary to determine some relationship between the doses to be expected from the different radiation types. The Conference minutes record an agreement to define the Relative Biological Effectiveness as the "ratio between the quantities of different types of radiation (measured in ergs per gram) required to produce the same biological effect." It was further agreed that the RBE of radium gamma rays should be used as a standard and therefore considered unity. Since no RBE is given for other gamma rays (except 200-kv X rays), all are assigned

a RBE of one in shielding work. The complete table from the Conference minutes is as follows:

Table 9 Relative Biological Effectiveness

Type of Radiation	RBE	
	Bone Marrow	Skin
Alpha	20	
Beta	1	
Gamma (radium)	1	1
X rays (200-kv)	1	1.5
Fast neutrons of < 20 Mev	10	
Slow neutrons	5	
Protons	10	

The RBE, however, does not yield at once the equivalence of fluxes of the various radiation types, since the energy deposited varies considerably with many factors, such as neutron energy, angle of arrival, size of body irradiated, etc. As a consequence the tolerance specification is the result of much calculation and is based on many arbitrary assumptions.

The conference agreed to specify dosage in terms of "roentgens equivalent physical," which has subsequently been dubbed the rep" and which represents that amount of radiation depositing 93 ergs per gram of tissue. The rep is very close to the roentgen, which is defined in terms of energy deposited in dry air. No distinction between the two need be made in shielding work at present.

The most important specification is the amount of gamma (standard) radiation to be tolerated. For civilian occupation this was chosen to be 0.3 rep

per 40-hr week, with no specification on how the dose is to be distributed during the week. For purposes of shield design the radiation rate in a laboratory is never allowed to exceed .0075 rep/hr, and usually the limit is kept lower than this by about a factor of 10 to insure negligible instrument background. Figure 6, page 45, can be used to convert this dose rate to photon flux. The allowed dose rate applies to that part of the body which is most intensely irradiated except that doses limited to the hands and forearm can exceed the normal dose by a factor of five.

The neutron situation is not quite so simple, since there are many ways in which the energy can be deposited in the flesh. Dr. Walter S. Snyder, of ORNL, has calculated the tolerance dose both for thermal⁽⁵¹⁾ and fast⁽⁵²⁾ neutrons. The calculation for thermal neutrons is probably fairly accurate and will not be expected to be changed by subsequent work. The data available to Snyder on differential cross sections for the fast-neutron calculations may indicate somewhat different values. Furthermore, Snyder's calculation applies to a collimated beam of neutrons incident normally on a 30-cm-thick slab of meat. Inclusion of radiation from other angles may alter the result. This particular point is of interest in specifying the dose inside an airplane crew compartment where the neutrons arrive from all directions. The dose for this case is much more difficult to specify.

For shielding work, Snyder's⁽⁵³⁾ results will serve admirably and are reported in the following table:

Table 10 Neutron Fluxes Biologically Equivalent
to 0.3 rep of Gamma Rays per 40-hr Week

Neutron Energy	Flux, n/cm ² /sec
Thermal	1800
5 kv	1640
0.5 Mev	82
2.5 Mev	38
5 Mev	26
10 Mev	26

At the Chalk River conference it was also agreed that "no manifest permanent injury is to be expected from a single exposure of the whole body to 25 r or less, with the possible exception of pregnant women." The Lexington Project⁽⁵⁴⁾ used 25 r as the dose to be given to the crew of the nuclear-powered airplane. This dose has been used so consistently since then that it has acquired venerability, if not authenticity. Recently it has been questioned by a number of organizations interested in nuclear-powered flight and a program to determine the proper tolerance is expected to be undertaken soon. It is interesting to note that while 1 r/hr (the aircraft mission is assumed to last 25 hr) is taken as the "military dose," nevertheless the U.S. Navy plans to expose its crew to little more than the usual laboratory tolerance dose.

EPB:lg
3/7/52

Revised
EPB:ms
10/9/52

REFERENCES (continued from Part I)

- (25) Report of the Shielding Board for the ANP Program, ANP-53, Appendix A, October 16, 1950.
- (26) The Aircraft Nuclear Propulsion Project Quarterly Progress Report for Period Ending May 31, 1950, P. 43, ORNL-768.
- (27) E. P. Blizard, "ORNL Shielding Program - An Outline," ORNL C.F. 48-12-9, November 30, 1948.
- (28) E. P. Blizard, C. E. Clifford, and J. Cassidy, "Shielding Efficiency of an Oxychloride-Iron Concrete - Comparison with Hanford Shield," P. 3 and Fig. 9, ORNL-32, June 7, 1948.
- (29) W. K. Ergen and C. E. Clifford, "Experimental Facilities and Equipment Used in the 1948 'NEPA' Bulk Shielding Tests," ORNL C.F. 49-8-80, July 20, 1949.
- (30) T. A. Welton, "Analysis of Shielding Data," LP-141, September 2, 1948. Note that the fission plate source is incorrectly shown in this report to be at the inner opening of the core hole. It was in fact fastened to the inner surface of the shield sample "plug." For a description of the experiment and accurate picture of the sample see the Physics Division Quarterly Report, ORNL-159, P. 106 ff., and for the data see the next quarterly report, ORNL-228, P. 81.
- (31) H. P. Sleeper, Jr., "A Critical Review of ORNL Shield Measurements: Neutron Attenuation," ORNL-436, December 21, 1949; also W. K. Ergen and C. E. Clifford, "Neutron and Gamma Attenuation through Tungsten Carbide and Boron Carbide," ORNL-435, December 9, 1949.
- (32) E. P. Blizard et al., "Reactor Shielding with an Iron Aggregate Concrete - Comparison with Ordinary Concrete," ORNL-209, March 16, 1949.
- (33) C. E. Clifford, "The ORNL Shield Testing Facility," ORNL-402, November 4, 1949, or see his article in "Theoretical and Practical Aspects of Shielding," ORNL-710, P. 193, September 29, 1950.
- (34) W. M. Breazeale, "The New Bulk Shielding Facility at ORNL," ORNL-991, May 8, 1951.
- (35) W. M. Breazeale, "A Low Cost Experimental Neutron Chain Reactor," ORNL-1105, November 21, 1951.
- (36) C. N. Rucker, "Proposal for a New Bulk Shield Testing Facility," ORNL C.F. 49-12-92, December 21, 1949.
- (37) "Supplement to Proposal for Bulk Shield Testing Facility," ORNL C.F. 50-2-19, February 6, 1950.
- (38) A. C. Rand, "Mechanical Features of the Brookhaven Shielding Facility," BNK 139/T-26, forthcoming.

- (39) H. Castle, H. Ibser, G. Sacher, and A. M. Weinberg, "The Effect of Fast Fission on k," CP-644, May 4, 1943.
- (40) F. H. Murray, "Fast Effects, Self-Absorption, Fluctuation of Ion Chamber Readings, and the Statistical Distribution of Chord Lengths in Finite Bodies," CP-2922, April 6, 1945.
- (41) S. Kushneriuk, "Absorption of Gamma Rays by Homogeneous Cylinders Containing Uniform Source Distributions," TPI-46, May 6, 1947.
- (42) Report of the Shielding Board, ANP-53, Appendix B, October 16, 1950; also see Welton and Albert, WAPD-15, November 30, 1950.
- (43) Report of the Shielding Board, ANP-53, Appendix F, October 16, 1950; (see in particular the table on P. 163).
- (44) Aircraft Nuclear Propulsion Project Quarterly Progress Report for Period Ending December 10, 1950, ORNL-919, P. 105, February 26, 1951.
- (45) Unpublished data by G. S. Hurst; also "A Method of Pulse Integration Using the Binary Scaling Unit," by F. M. Glass and G. S. Hurst, February or March issue of *Rev. Sci. Instruments*; G. S. Hurst, "A Proportional Counter Method of Measuring Fast Neutron Dose," C.F. 51-4-122.
- (46) N. M. Dismuke and M. R. Arnette, "Age to Thermal Energy (.025 e.v.) of Fission Neutrons in H₂O-Al Mixtures," Mon P-219, December 3, 1946. See also L. W. Nordheim, G. Nordheim, and H. Soodak, CP-1251; R. E. Marshak, MT-17; A. M. Weinberg, ORNL C.F. 48-9-128, P. 39; *Mathematics Panel Quarterly*, ORNL-888; and *Mathematics Panel Quarterly*, ORNL-1091.
- (47) B. O. Peirce, "Table of Integrals."
- (48) E. Jahnke and F. Emde, "Table of Functions."
- (49) E. P. Blizard and H. L. F. Enlund, "Thermal Flux in a Water Shield," *The Physics Division Quarterly Progress Report for Period Ending December 20, 1951*, ORNL-1216.
- (50) Minutes of the Permissible Doses Conference, Chalk River, Canada, September 29, 30, 1949, Report No. R.M.-10.
- (51) W. S. Snyder, "Calculations for Maximum Permissible Exposure to Thermal Neutrons," *Nucleonics*, 6, No. 2, PP. 46-50, February 1950.
- (52) W. S. Snyder - Private Communication and forthcoming ORNL report.
- (53) W. S. Snyder's data is reported in the Monthly Progress Report of ORNL, ORNL-1282, P. 20.
- (54) The Report of the Lexington Project, Lex-P-1.

- - - -